Clim Dyn (2017) 49:2569–2583
DOI 10.1007/s00382-016-3469-9

Permafrost degradation and associated ground settlement estimation under 2 °C global warming

Donglin Guo[1,2,3] · **Huijun Wang**[1,4]

Received: 28 July 2016 / Accepted: 26 November 2016 / Published online: 2 December 2016

Abstract Global warming of 2 °C above preindustrial levels has been considered to be the threshold that should not be exceeded by the global mean temperature to avoid dangerous interference with the climate system. However, this global mean target has different implications for different regions owing to the globally nonuniform climate change characteristics. Permafrost is sensitive to climate change; moreover, it is widely distributed in high-latitude and high-altitude regions where the greatest warming is predicted. Permafrost is expected to be severely affected by even the 2 °C global warming, which, in turn, affects other systems such as water resources, ecosystems, and infrastructures. Using air and soil temperature data from ten coupled model intercomparison project phase five models combined with observations of frozen ground, we investigated the permafrost thaw and associated ground settlement under 2 °C global warming. Results show that the climate models produced an ensemble mean permafrost area of 14.01×10^6 km^2, which compares reasonably with the area of 13.89×10^6 km^2 (north of 45°N) in the observations. The models predict that the soil temperature at 6 m depth will increase by 2.34–2.67 °C on area average relative to 1990–2000, and the increase intensifies with increasing latitude. The active layer thickness will also increase by 0.42–0.45 m, but dissimilar to soil temperature, the increase weakens with increasing latitude due to the distinctly cooler permafrost at higher latitudes. The permafrost extent will obviously retreat north and decrease by 24–26% and the ground settlement owing to permafrost thaw is estimated at 3.8–15 cm on area average. Possible uncertainties in this study may be mostly attributed to the less accurate ground ice content data and coarse horizontal resolution of the models.

Keywords Permafrost degradation · Ground settlement · 2 °C global warming · CMIP5

✉ Donglin Guo
guodl@mail.iap.ac.cn

[1] Nansen-Zhu International Research Center, Institute of Atsmospheric Physics, Chinese Academy of Sciences, P. O. Box 9804, Beijing 100029, China

[2] Collaborative Innovation Center on Forecast and Evaluation of Meteorological Disasters (CIC-FEMD), Nanjing University of Information Science & Technology, Nanjing 210044, China

[3] Joint Laboratory for Climate and Environmental Change, Chengdu University of Information Technology, Chengdu 610225, China

[4] Key Laboratory of Meteorological Disaster, Ministry of Education (KLME)/ Collaborative Innovation Center on Forecast and Evaluation of Meteorological Disasters (CIC-FEMD), Nanjing University of Information Science & Technology, Nanjing 210044, China

1 Introduction

The global climate has experienced warming during the last century, and it is projected to continue to warm in the next 100 years (Collins et al. 2013). Climate warming is expected to affect geophysical, biological, and socio-economic systems (Schneider et al. 2007; Wang and Sun 2009; Liu et al. 2012; Li et al. 2015; Wang et al. 2015). To prevent the dangerous effects of climate warming, policy makers and the scientific community consider that society should maintain the global mean warming below 2 °C

relative to preindustrial temperatures (UNFCCC 2010, 2015). However, climate warming has not been globally uniform. Higher warming is observed and projected to occur in higher northern latitudes and high-altitude areas (Guo and Wang 2012; Collins et al. 2013; Hartmann et al. 2013; Zhou et al. 2014, 2016). Therefore, regional climate changes are expected to differ under this target of global warming of 2 °C.

Permafrost is defined as the ground where soil temperature remains at or below 0 °C for at least two consecutive years. In the Northern Hemisphere, permafrost extent is estimated to be approximately 22.79×10^6 km^2, which is equivalent to approximately 1/4 of the Northern Hemisphere land area. It is estimated that permafrost soils in the Northern Hemisphere store approximately $11.37–36.55 \times 10^3$ km^3 of ground ice (Zhang et al. 1999). The ablation of the ground ice will largely affect hydrology and water resources (Guo et al. 2012; Lan et al. 2015; Liljedahl et al. 2016). In addition, the freezing and thawing processes of the surface layers of permafrost regulate the variations of soil and surface water and heat, which further strongly affect soil biogeochemical cycles, surface energy budgets, local hydrological processes, and vegetation (Yang et al. 2010, 2014; Guo et al. 2011a, b; Li and Chen 2013; Yi et al. 2014; Qin et al. 2014). Besides, as a large carbon pool, permafrost soils store approximately twice the carbon presented in the current atmosphere (Zimov et al. 2006; Schuur et al. 2009). The release of the carbon caused by permafrost degradation may intensify climate warming (Schuur et al. 2009, 2015; Koven et al. 2011; Burke et al. 2013). From the human perspective, the ablation of ground ice in permafrost can result in the settlement of the ground surface, which will affect the stability of permafrost-underlain infrastructures (Nelson et al. 2002; Guo and Sun 2015).

Despite these effects mentioned above, permafrost is widely distributed in high-latitude and high-altitude regions where the greatest warming is predicted to occur. Furthermore, as defined by the ground temperature, permafrost is potentially sensitive to climate change (Anisimov et al. 2001; Guo and Wang 2013, 2014). Clearly, the Earth's permafrost is likely easy to degrade in response to global climate warming. Thus, it is expected that permafrost will be significantly affected even at the relatively moderate target of 2 °C global warming, which, in turn, affects other systems such as hydrology and water resources, ecosystems, human infrastructures, and climate change.

Because of growing concerns, research efforts have concentrated on investigating changes in regional-climate-sensitive systems during 2 °C global warming relative to preindustrial temperatures (Kaplan and New 2006; Giannakopoulos et al. 2009; Meinshausen et al. 2009; Jiang and Fu 2012; May 2012; Vautard et al. 2014; Sui et al. 2015). Kaplan and New (2006) investigated the effect of 2 °C global warming on the Arctic climate and vegetation cover. Their results showed that the Arctic forest extent increases by 55% with a corresponding decrease of 42% in the tundra area, which is significant. Climate change and associated impact in the Mediterranean basin under the 2 °C global warming scenario were investigated using the Hadley Centre Coupled Model version 3 (HadCM3) (Giannakopoulos et al. 2009). More recently, Jiang and Fu (2012) analyzed the climate change over China under the 2 °C global warming scenario using an ensemble of 16 GCM simulations and reported that the area-averaged annual temperature and precipitation in China increases by 2.7–2.9 °C and 3.4–4.4%, respectively, relative to the period 1890–1900. The European climate under the 2 °C global warming scenario was also analyzed using an ensemble of 15 regional climate simulations (Vautard et al. 2014). Most of Europe will experience higher warming than the global average, and robust changes in the mean and extreme temperatures, precipitation, and wind and surface energy budgets are expected. Nevertheless, permafrost change and the associated ground settlement amount under the 2 °C global warming have not been fully assessed.

Although some studies have referred to the simulation of permafrost change in response to climate warming (Anisimov and Nelson 1996, 1997; Stendel and Christensen 2002; Lawrence et al. 2008, 2012; Zhang et al. 2008; Koven et al. 2013; Slater and Lawrence 2013; Guo and Wang 2016a, b; Liu and Jiang 2016), they did not focus on spatial and quantitative changes in permafrost under the 2 °C global warming, which are important for looking at the global warming threshold of 2 °C from permafrost change perspective. Some studies have also referred to thaw settlement of permafrost (Nelson et al. 2001, 2002; Anisimov and Reneva 2006; Zhang and Wu 2012), but they mostly presented settlement hazard zonation with relative risk grade (stable, low, moderate, and high risk) rather than amount of the ground settlement. Specific settlement amount of the ground surface is important for flexible evaluation of permafrost-underlain infrastructure stabilization.

The focus of the present study is on quantitatively assessing the permafrost thaw and associated settlement amount of the ground surface resulting from the 2 °C global warming using air and soil temperature data from 10 CMIP5 models and observations of frozen ground. Before assessing, the time at which the global mean temperature will increase by 2 °C relative to the preindustrial level from the used 10 CMIP5 models is estimated. In addition, a validation of the simulations of soil temperature, active layer thickness (ALT), and permafrost area from climate models is performed based on in situ observations and the Circum-Arctic permafrost map (Brown et al. 1997).

2 Data and methods

2.1 Data

Monthly air and soil temperature data during the historical and future periods were obtained from CMIP5 simulations (http://cmip-pcmdi.llnl.gov/cmip5/). Two representative concentration pathways (RCPs, usually refer to the portion of the concentration pathway extending up to 2100) were used: RCP4.5 [an intermediate stabilization pathway in which radiative forcing is stabilized at approximately 4.5 W m^{-2} (approximately 650 ppm CO_2 equivalent) after 2100, Moss et al. 2010] and RCP8.5 [an high pathway in which radiative forcing is stabilized at approximately 8.5 W m^{-2} (approximately 1370 ppm CO_2 equivalent) after 2100, Moss et al. 2010]. Ten climate models (CCSM4, CESM1-CAM5, GFDL-ESM2g, MIROC5, MIROC-ESM, MPI-ESM-LR, MPI-ESM-MR, MRI-CGCM3, NorESM1-M, and NorESM1-ME) were selected obeying the following restrictions. (1) Soil temperature are not available for some climate models. (2) Climate models with soil depths shallower than 6 m were not selected in terms of the fact that inclusion of deeper soil tends to improve simulation of frozen ground (Lawrence et al. 2008). These models involve soil freezing and thawing processes and multiple snow layers in the land surface components (e.g., Takata et al. 2003; Lawrence et al. 2011). Most of these models also involve soil organic matter (e.g., Lawrence et al. 2011). The basic features of the ten models are presented in Table 1, and additional details regarding the simulations can be found in Taylor et al. (2012). The CMIP5 simulation data are derived from the Earth System Grid Federation (ESGF) gateway (http://pcmdi9.llnl.gov/esgf-web-fe/). The data have been widely used in simulating and predicting

Table 1 Details of the models

Model name	Resolution (°lon × °lat)	Soil temperature at 1 m depth (°C)	Soil temperature at 6 m depth (°C)	Land model	No. of soil layers	Soil depth (m)	Snow layer	Organic matter	Model reference
CCSM4	0.9×1.125	−4.06	−4.16	CLM4	15	35.18	Multilayer	Yes	Lawrence et al. (2012), Gent et al. (2011)
CESM1-CAM5	0.9×1.125	−5.97	−5.99	CLM4	15	35.18	Multilayer	Yes	Lawrence et al. (2012), James et al. (2013)
GFDL-ESM2g	2.0×2.5	−10.67	−10.76	LM3	23	8.75	Multilayer	No	Dunne et al. (2012)
MIROC5	1.4×1.4	−9.58	−9.69	MATSIRO	6	9.0	Multilayer	No	Takata et al. (2003), Watanabe et al. (2010)
MIROC-ESM	2.81×2.81	−5.93	−6.05	MATSIRO	6	9.0	Multilayer	No	Takata et al. (2003), Watanabe et al. (2011)
MPI-ESM-LR	1.87×1.87	−9.05	−9.04	JSBACH	5	6.98	Multilayer	Yes	Giorgetta et al. (2013)
MPI-ESM-MR	1.87×1.87	−8.37	−8.33	JSBACH	5	6.98	Multilayer	Yes	Giorgetta et al. (2013)
MRI-CGCM3	1.12×1.12	−4.57	−4.62	HAL	14	8.5	Multilayer	No	Yukimoto et al. (2012)
NorESM1-M	1.87×2.5	−6.08	−6.14	CLM4	15	35.18	Multilayer	Yes	Lawrence et al. (2012), Bentsen et al. (2013)
NorESM1-ME	1.87×2.5	−6.46	−6.45	CLM4	15	35.18	Multilayer	Yes	Lawrence et al. (2012), Tjiputra et al. (2013)

Soil temperatures are mean values averaged in the simulated present-day permafrost area for 1981–2000. The soil depth refers to the maximum depth with soil temperature data rather than the depth prescribed in the models.

permafrost dynamics and climate change (Koven et al. 2013; Slater and Lawrence 2013; Hua et al. 2014; Guo and Sun 2015; Guo and Wang 2016b).

In situ site observations of the soil temperature at depths of 1 and 6 m and the ALT were also used to validate the results of the simulations. The soil temperature observations were obtained from (1) Russian historical soil temperature (RHST) measurements (Zhang et al. 2001) at 1 m depth and (2) the International Polar Year thermal state of permafrost (IPY-TSP) at 6 m depth (Romanovsky et al. 2010; Romanovsky 2010) (Table 2). The RHST data cover the total period from 1882 to 1990 but are not continuous. Many stations have data beginning in the 1930s and 1950s. Moreover, not all stations have data through 1990. The data were obtained at depths ranging from 0.02 to 3.2 m. In this study, the 1980–1990 average of the RHST data were used to validate the present-day simulated soil temperature at 1 m depth during the corresponding period. It should be mentioned that these HRST data may be systematically biased because the measurements were generally made on bare soils in which surface organic layers had been removed for agricultural purposes (Gilichinsky et al. 1998). In spite of this issue, the data still were used due to the scarcity of soil temperature observations in permafrost region. The IPY-TSP data cover the period of 2007–2008 with a total measured depth of 0–100 m, but this is not the case for all stations. These data were used to validate the simulated soil temperature at 6 m depth during the corresponding period. Because soil temperature at 6 m depth have weak inter-annual variations (Wu and Zhang 2008), the validation based on the period of 2007–2008 is valid although climate models are not supposed to accurately replicate the inter-annual climate variations. For both observations mentioned above, the soil temperatures at the depths of interest (1 and 6 m) were not directly measured at all sites included in the corresponding data bases; they were estimated using simple linear interpolation between known values. These observations are reliable and have been used to validate the results from climate models (Lawrence et al. 2012; Koven et al. 2013).

ALT observations were also obtained from (1) the Circumpolar active layer monitoring (CALM) network (Brown et al. 2000) and (2) the historical active layer thickness calculated from soil temperature observations at 31 Russian sites (AL_RHST) (Zhang et al. 2006) (Table 2). The CALM data cover the period of 1990–2015, but not all stations have data for the entire period. The data for 1990–2000 were used in this study for validation of the present-day simulation results. The AL_RHST data cover the period of 1930–1990 and the data for 1980–1990 were used for validating the present-day simulation results. These two datasets were first averaged over their recorded period at each station and then respectively compared to the simulated ALT for the corresponding period. These ALT observations also are reliable and have been used to assess the climate model results (Lawrence et al. 2012; Koven et al. 2013).

Permafrost area and ground ice in permafrost were obtained from the Circum-Arctic map of permafrost and ground ice conditions (Brown et al. 1997), which are perhaps the best available data on the distribution of permafrost and ground ice. The data were used to validate the present-day simulations of the permafrost area and estimate the settlement of the ground surface. The data are archived at a resolution of 0.5° longitude × 0.5° latitude at http://nsidc.org/data/docs/fgdc/ggd318_map_circumarctic/index.html. Permafrost is classified into continuous, discontinuous, isolated, and sporadic; nevertheless, it is believed that GCMs generally can only identify continuous and discontinuous permafrost due to their coarse resolutions (Burn and Nelson 2006). Thus, only these two types were used in the validation of the model results of this study. It should be mentioned that this approach is resolution-dependent, which may be not true for higher-resolution model. The ground ice content of the permafrost refers to relative abundance of ground ice, which is given in 3% volumes: 0–10, 10–20, and >20%. Consequently, only the corresponding range in the settlement of the ground surface can be estimated, i.e., minimum and maximum settlement, shown in Sect. 3.3. Notably, for the areas with ground ice content >20%, the maximum ground ice content is unclear. In order to obtain maximum value of settlement, an upper bound value of ground ice content of 100% is used in this study. By doing this, the estimated maximum settlement is amplified in these areas to some extent, although these areas are small, as shown in Sect. 3.3.

Table 2 Summary of the information of the observed data used to validate climate model results

Data	Name	Depth (m)	Period of used data	Reference
Soil temperature	RHST	1.0	1980–1990	Zhang et al. (2001)
	IPY-TSP	6.0	2007–2008	Romanovsky et al. (2010), Romanovsky (2010)
Active layer thickness	CALM		1990–2000	Brown et al. (2000)
	AL_RHST		1980–1990	Zhang et al. (2006)

2.2 Methods

The settlement index (I_s), developed by Nelson et al. (2002), was used to estimate the settlement amount of the ground surface owing to permafrost thaw,

$$I_s = \Delta Z_{al} V_{ice} \quad (1)$$

where ΔZ_{al} is the relative change in the ALT and V_{ice} is the ground ice content of volumetric proportion. This index considers ALT and ground ice as the most important factors of the permafrost. The assumption in Eq. (1) is that liquid water generated by melting ground ice can timely drain away from the study site, and the associated settlement of the ground surface is proportional to the thickness of the melted ground ice. In Eq. (1), I_s is a dimensionless index. Thus it cannot express a certain settlement amount that is flexible for application. Guo and Sun (2015) used the actual increases (unit: m) to replace the originally relative change in the ALT. Consequently, the index I_s represents the certain settlement amount of the ground surface, with a unit of meters. In this study, the above modification is also performed. The ground ice content, required by Eq. (1), was directly derived from the Circum-Arctic map of permafrost and ground ice conditions (Brown et al. 1997), and the ALT was calculated using the soil temperature from the climate models. The method of calculation of the ALT can be seen in the next paragraph.

Permafrost was identified as the ground where at least one soil layer in the upper 3.5 m had monthly soil temperature below 0 °C for at least 24 consecutive months. The permafrost is near-surface permafrost because the depth of 3.5 m was used as in Lawrence et al. (2008). The ALT was computed as the maximum depth of thaw for permafrost ground over the course of the year (Lawrence et al. 2008). As shown in Table 1, the climate models show several different numbers of soil layer and spatial resolutions. In this study, the temperature of the soil layers of each model were first linearly interpolated to evenly spaced layers with thickness of 0.1 m before they were used to calculate the permafrost and ALT. The interpolation is allowed due to the fact that soil temperature generally show a linear relationship with depth (Koven et al. 2013). For the spatial resolution, together with all simulated data from the CMIP5 models, the permafrost and ground ice data were interpolated with the resolution of 0.9° longitude × 1.125° latitude of CCSM4 for homogenous calculation and comparison.

Not all the CMIP5 models were run from the start of the preindustrial period (1750 or 1850) (Schneider et al. 2007). Some models did not produce data for the preindustrial period. To correct this, Schneider et al. (2007) proposed that the 2 °C warming above preindustrial levels corresponded to 1.4 °C warming above the 1990–2000 levels. Therefore, this study used the 1.4 °C warming relative to the period of 1990–2000 to estimate the time of the 2 °C global warming. The same approach was also used in Lang and Sui (2013).

In addition, in this study, the 21 years mean permafrost conditions centered on the 2 °C global warming times (identified in the following Sect. 3.1) were first calculated, and then their differences from the 1990–2000 mean level were taken as changes in permafrost and the associated ground settlement under the 2 °C global warming.

3 Results

3.1 Time of the 2 °C global warming

Time series of the global mean air temperature anomalies of each model are shown in Fig. 1, which are smoothed with the 21-year moving average as in Kaplan and New (2006). It should be mentioned that, in the RCP2.6 scenario, only CESM-CAM5 and MIROC-ESM temperature reach 1.4 °C in 2033 and 2035, respectively. The ensemble mean air temperature of all models is always lower than 1.4 °C until the end of the simulation. Therefore, the RCP2.6 scenario is not considered in this study. The air temperature of all models except GFDL-ESM2G reached 1.4 °C in 1950–2090 under the RCP4.5 scenario. The corresponding times are between 2030 and 2054, if GFDL-ESM2G is not considered. The ensemble mean temperature reached 1.4 °C in 2045, which is taken as the time of the 2 °C global warming. Under the RCP8.5 scenario, the air temperature of all models reached 1.4 °C in 1950–2090, with corresponding time of 2027–2051. The ensemble mean temperature reached 1.4 °C in 2037, which is taken as the time of the 2 °C global warming in this scenario.

In order to validate the times of the 2 °C global warming identified above, we compare them with the previous results. Jiang and Fu (2012) reported 2046 as the time of the 2 °C global warming under the A1B scenario. For comparison, we calculated 2045 under the RCP4.5 scenario, which is similar to the A1B scenario. When the median is calculated to compare the time of the 2 °C global warming in Vautard et al. (2014), we calculated 2049 (RCP4.5) and 2039 (RCP8.5), which are comparable to 2050 (RCP4.5) and 2042 (RCP8.5). Thus, the estimated times in this study is appropriate.

The mean air temperature change in the permafrost region is compared to the global mean temperature. As shown in Fig. 2, the air temperature in the permafrost region increases by 2.3–3.8 °C (RCP4.5) and 2.4–3.5 °C (RCP8.5) relative to 1990–2000, when the global mean temperature increases by 1.4 °C. The best estimate for the global mean temperature increase from the preindustrial period to 1990–2000 is 0.6 °C (Schneider et al. 2007).

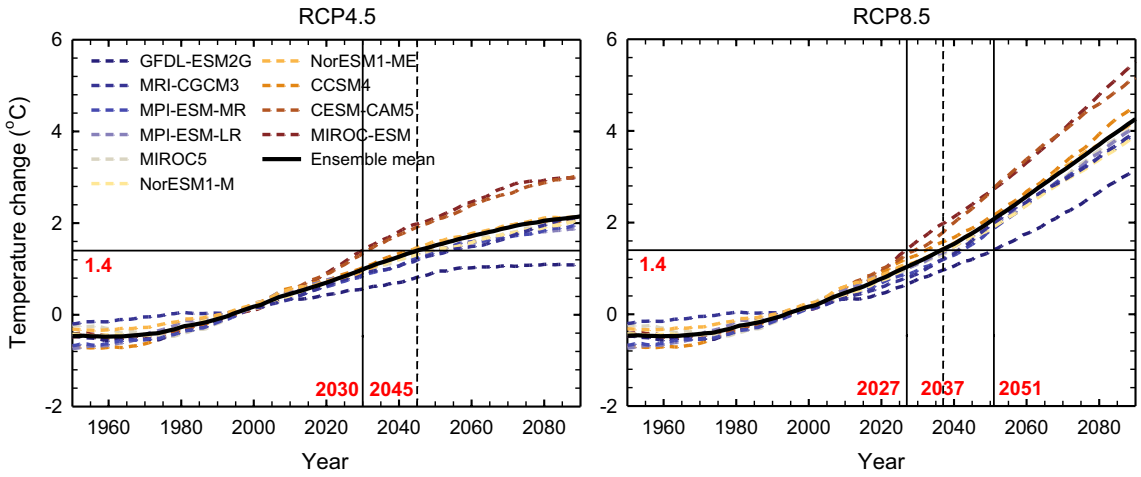

Fig. 1 Global mean annual air temperature anomalies from 1950 to 2100 under the RCP4.5 and RCP8.5 scenarios, relative to 1990–2000, and smoothed with the 21-year moving average. *Vertical lines* refer to the earliest (*solid*), latest (*solid*), and average (*dashed*) time at which the global air temperature anomaly exceeds 1.4 °C in the ten climate models. The 1.4 °C warming relative to 1990–2000 is used instead of the 2 °C warming relative to the preindustrial period because the 1.4 °C warming above the 1990–2000 levels corresponds to a 2 °C warming above the preindustrial levels (Schneider et al. 2007)

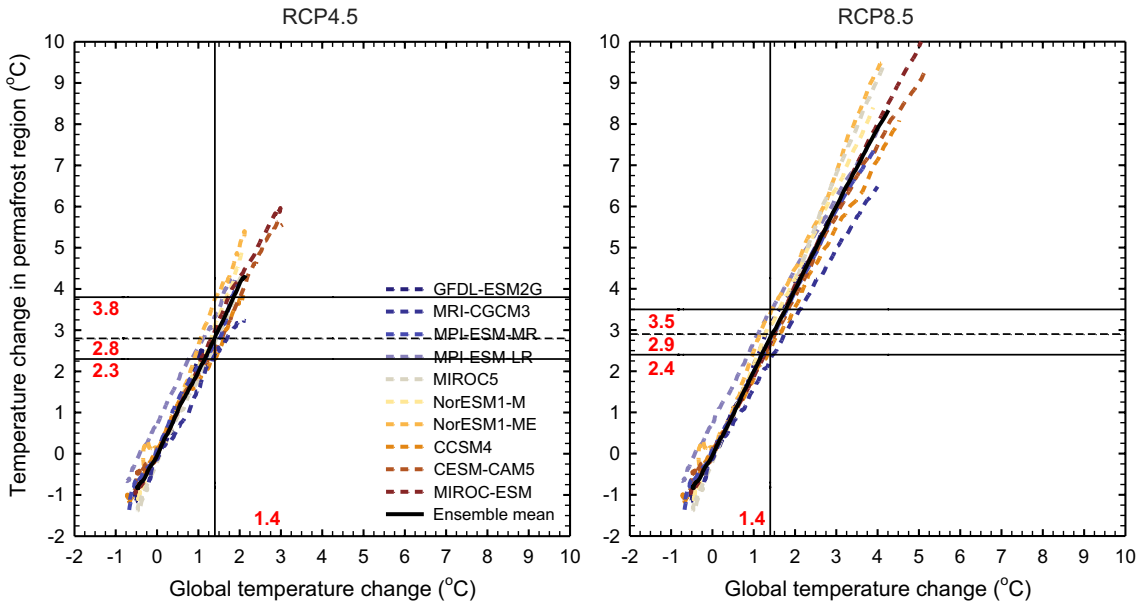

Fig. 2 Comparison of air temperature change in global and permafrost regions from 1950 to 2100 under RCP4.5 and RCP8.5 scenarios, relative to 1990–2000, and smoothed with the 21-year moving average. *Horizontal lines* denote the minimum (*solid*), maximum (*solid*), and average (*dashed*) temperature change predicted for the permafrost region when the 21-year mean global air temperature anomaly reaches 1.4 °C in the ten climate models

Moreover, the higher northern latitudes are observed to experience larger warming than the global mean (Hartmann et al. 2013). Therefore, using the preindustrial period as reference, the air temperature in the permafrost region increases by at least 2.9–4.4 °C (RCP4.5) and 3.0–4.1 °C (RCP8.5) when the global mean temperature reaches 2 °C. Such a relatively high warming is expected to significantly affect the permafrost.

3.2 Validation of the model results

The results from the CMIP5 models are validated based on in situ site observations. As shown in Fig. 3a, the spatial change pattern of the simulated soil temperature at 1 m depth agrees with the site observations. The pattern and site observations suggest a consistent poleward change of soil temperature from warm to cold. This also holds for the

soil temperature at 6 m depth (Fig. 3b). Six statistical indices (mean bias, mean absolute, root mean square error, spatial correlation coefficient, percent bias, and Nash-Sutcliffe efficiency) regarding spatial similarities between the gridded simulations and corresponding site observations are shown in Table 3. The mean absolute bias and spatial correlation coefficient is 1.90 °C and 0.79, respectively, for soil temperature at depth of 1 m, and 1.40 °C and 0.86, respectively, for soil temperature at depth of 6 m (Table 3). For the ALT, the simulated spatial pattern is also in good agreement with the site observations, presenting a poleward change for the active layer from thick to thin (Fig. 3c, d). The mean absolute bias and spatial correlation coefficient is 0.49 m and 0.36, respectively, for ALT compared to CALM

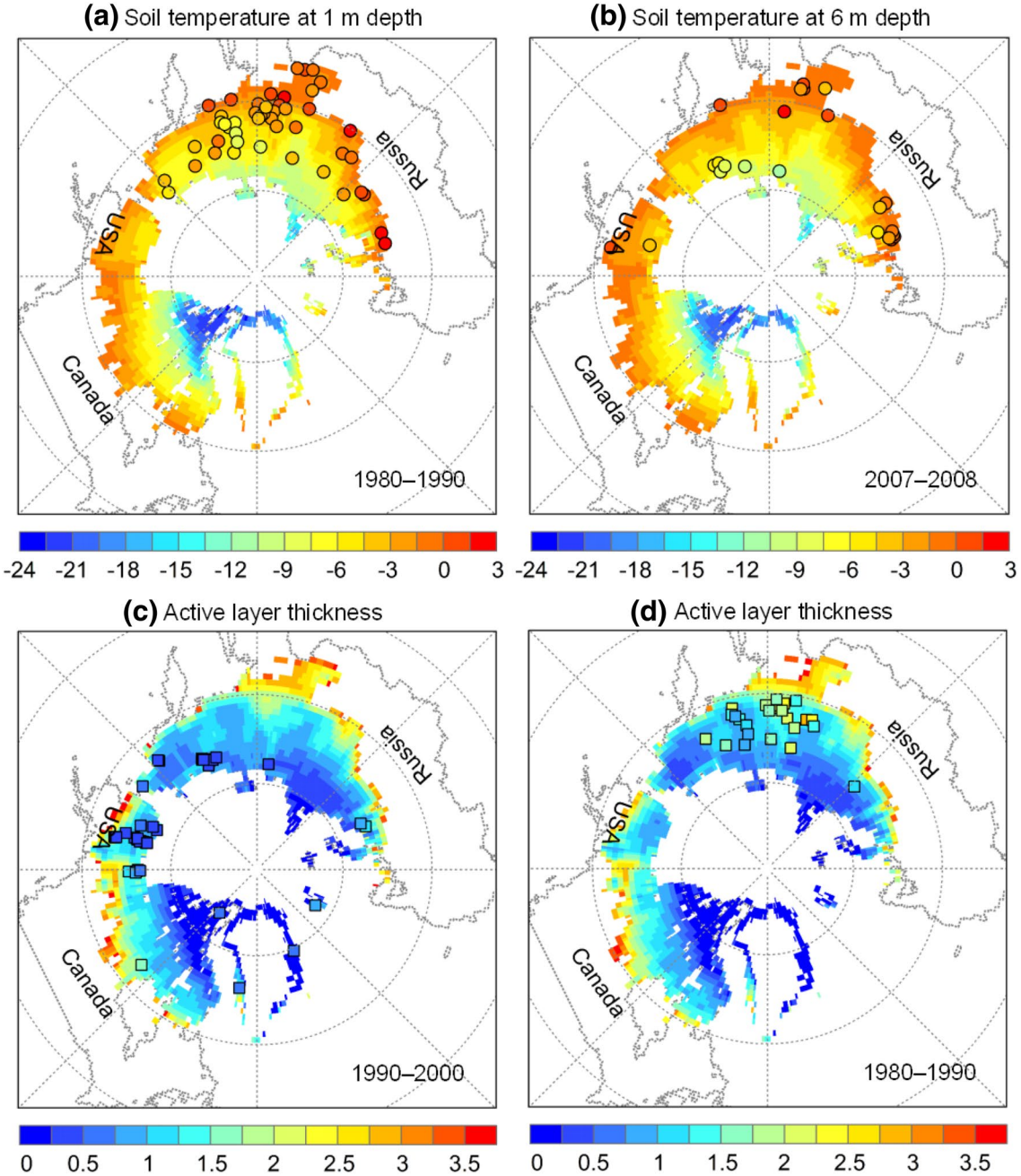

Fig. 3 Comparison of the present-day simulated ensemble-mean soil temperature (°C, *shaded color*) at depth of 1 m (**a**), for 1980–1990 and 6 m (**b**), for 2007–2008, and active layer thickness (m, *shaded color*) for 1990–2000 (**c**) and for 1980–1990 (**d**) with observations (*circles* for soil temperature and rectangles for active layer thicknesses). *Panels* **c** and **d** are based on CALM and AL_RHST observations, respectively. The three countries (Russia, Canada, and the USA), containing permafrost, are outlined by the gray dashed lines

Table 3 Statistics of spatial similarities between the gridded simulations and corresponding site observations for soil temperature at 1 and 6 m depths and active layer thickness

Index	Soil temperature at 1 m depth	Soil temperature at 6 m depth	Active layer thickness (CALM)	Active layer thickness (AL_RHST)
Mean bias (°C)	−1.53	−0.34	0.39	−0.42
Mean absolute bias (°C)	1.90	1.40	0.49	0.49
Root mean square error (°C)	2.20	1.80	0.55	0.63
Spatial correlation coefficient	0.79	0.86	0.36	0.50
Percent bias (%)	73	12	62	24
Nash-Sutcliffe efficiency	0.30	0.72	−2.27	−0.53

All correlation coefficients exceed the 95% significance level

observations, and 0.49 m and 0.50, respectively, for ALT compared to AL_RHST observations (Table 3). Notably, when calculating the mean biases and spatial correlation coefficients, if a model grid cell contains more than one borehole site, the site observations are first averaged, as the "observed value" of this grid cell, and then the "observed value" is compared to the simulated value of this grid cell. Despite this, all original borehole sites, however, are shown in Fig. 3a–d.

The comparisons suffer from scale mismatch because they are based on grid-mean simulations and individual site observations. In a grid cell area, the soil temperature and ALT may vary substantially (Lawrence et al. 2012). Furthermore, the borehole sites are typically located in warm plains and basins (Wu et al. 2010), which tends to favor high observed soil temperatures compared with the grid-mean simulations. In this study, the observed high soil temperatures are shown in Fig. 3a, b. Considering these issues in the comparison, the simulation results are reasonable.

The climate models yields a present-day (1980–2000 average) ensemble mean permafrost area of 14.01×10^6 km^2, which is quite close to the area of 13.89×10^6 km^2 (north of 45°N) in the observations, with a bias of 0.12×10^6 km^2 (Fig. 4). This area is taken as the "simulated present-day permafrost area" in this study. In this comparison, the observations were developed using the data derived from the period of 1960–1993 (Brown et al. 1997), whereas the simulated present-day permafrost area is averaged over the period of 1980–2000. This mismatch in the periods may contribute to the deviation. Overall, the models yielded a reasonable present-day permafrost extent.

Notably, the aforementioned biases in the simulated soil temperature, ALT, and permafrost extent contain the systematic biases (a type of bias that deviates by a fixed amount from the true value) of the models. These systematic biases can be removed when calculating permafrost change that is the differences of permafrost during the two periods. In other words, the biases in the validation does not mean that the same biases will exist in the following permafrost change analysis. Actually, biases can be smaller

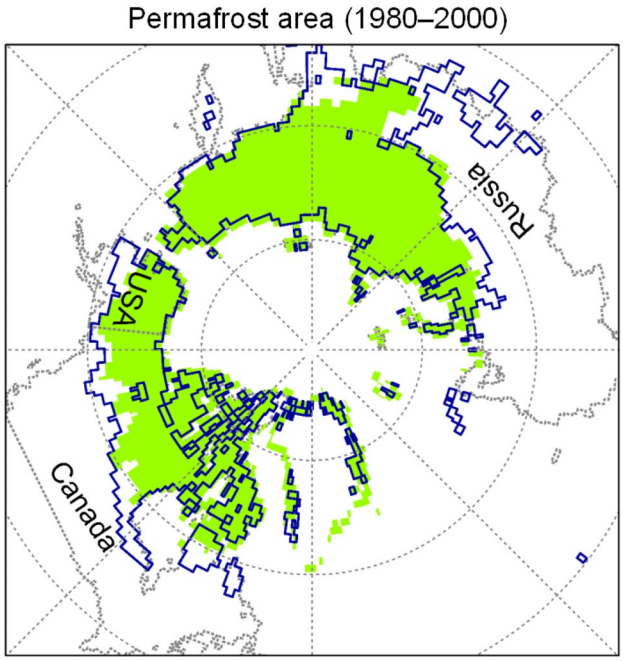

Fig. 4 Comparison of the present-day simulated ensemble-mean permafrost area (*shaded color*) for 1980–2000 with observations (areas outlined in *blue*). The three countries (Russia, Canada, and the USA), containing permafrost, are outlined by the *gray dashed lines*

in the permafrost change analysis due to the removal of the systematic biases, although it is difficult to estimate to what extent the biases become smaller.

3.3 Permafrost degradation and the ground settlement

In response to the 2 °C global mean warming relative to the preindustrial period, the soil temperature at 1 m depth increased relative to 1990–2000 with area means of 2.75 and 2.47 °C over the simulated present-day permafrost region under the RCP4.5 and RCP8.5 scenarios, respectively (Fig. 5a, b). From the spatial pattern, we can see that soil temperature increase gradually intensifies along with increasing latitude, and the largest increase is in the Canadian Archipelago. The pattern is similar to that from

ERA-Interim soil temperature change at 1 m depth from 1981 to 2005 (not shown).

The temperature in the deep soil layer can be taken as an indicator of the response of permafrost to long-term climate change (Xu et al. 2010). Therefore, the soil temperature change at depth of 6 m, the depth being integral and closest to the largest depth of 6.9 m of the simulated ensemble mean soil temperature, is also analyzed (Fig. 5c, d). The soil temperature increase at depth of 6 m is slightly lower than that at depth of 1 m, with area means of 2.67 and 2.34 °C over the simulated present-day permafrost region under the RCP4.5 and RCP8.5 scenarios, respectively. Similar to the situation at depth of 1 m, the soil temperature increase at 6 m depth also intensifies with increasing latitude, and the largest increases appear in the Canadian Archipelago.

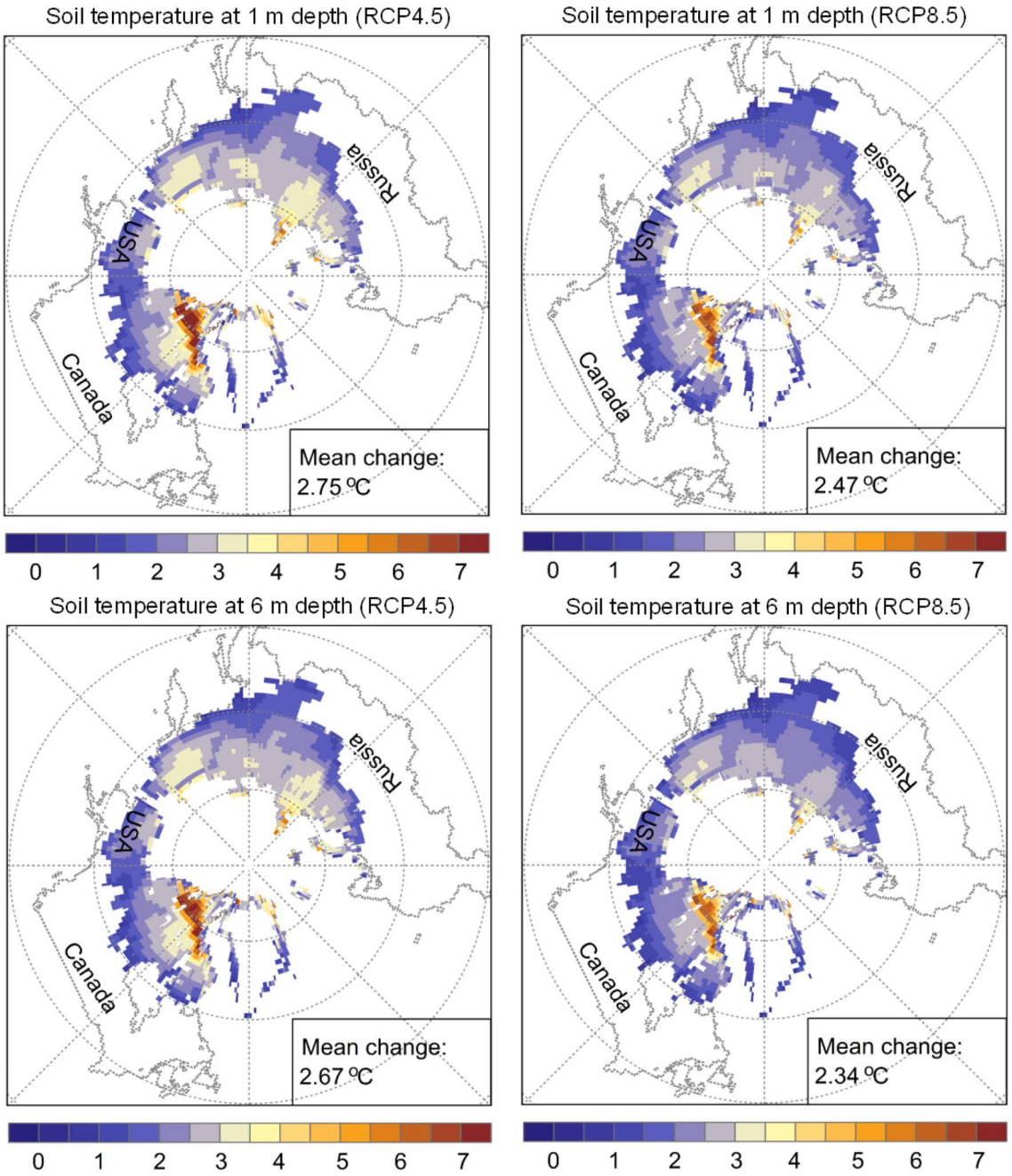

Fig. 5 Change in soil temperature (°C) at depths of 1 and 6 m between the 2 °C warming and 1990–2000 period under the RCP4.5 and RCP8.5 scenarios. Mean change denotes the area-averaged change. Three countries (Russia, Canada, and the USA), containing permafrost, are outlined by the *gray dashed lines*

Permafrost active layers thicken in response to the 2 °C global warming, ranging from 0 to 5.7 m (area mean: 0.45 m) and 0 to 5.2 m (area mean: 0.42 m) under the RCP4.5 and RCP8.5 scenarios, respectively (Fig. 6). Despite the spatial pattern of soil temperature change in which the increase intensifies with increasing latitude, the increase in the ALT weakens with increasing latitude. The reason can be explained as follows. As shown in Fig. 3a, permafrost thermal status distinctly cools with increasing latitude. Although the situation that soil temperature increase intensifies with increasing latitude plays a positive role in offsetting the cooling permafrost thermal status with increasing latitude, it is not sufficient to make the distinctly cooling permafrost thermal status with increasing latitude exceed the freezing point. In addition, the increase in ALT only depend on whether permafrost thermal status is above the freezing point. These two aspects jointly make that the increase in the ALT weakens with increasing latitude.

Permafrost area decreases by 26 and 24% under the RCP4.5 and RCP8.5 scenarios, respectively (Fig. 6). The losses primarily occur at the southern edge of permafrost region. Recall that the climate models can only identify continuous and discontinuous permafrost. In other words, these losses refer only to these two types of permafrost. Other types of permafrost, such as the isolated and sporadic permafrost, may suffer most losses, due to their relative warm properties at the southern edge of the entire permafrost region in the Northern Hemisphere.

The settlement of the ground surface owing to permafrost thaw is analyzed (Fig. 7). The minimum settlement is small in most of the permafrost region, except for a small number of grids at the southern edge of the permafrost region where it is relatively large. Over the entire permafrost area shown in Fig. 7, the minimum settlement ranges from 0 to 98 cm with area mean of 4 cm for RCP4.5 and from 0 to 104 cm with area mean of 3.8 cm for RCP8.5. The range between minimum and maximum settlement in most of the permafrost region is quite distinct, except in the Canadian Archipelago and northern Greenland where the maximum settlement is smaller than 1 cm. The maximum settlement ranges from 0 to 490 cm with area mean of 15 cm for RCP4.5 and from 0 to 520 cm with area mean of 14 cm for RCP8.5. From the spatial pattern, the maximum settlement decreases along with increasing latitude; however, this is not true for small areas (shown as rectangles), where relatively large values are seen at relatively high latitude. This is because the ground ice content is relatively large (>20%) in these small areas. In addition, as stated in Sect. 2.1, the ground ice content in these small areas is assigned the unrealistic maximum value of 100% when calculating the maximum settlement. Thus, the maximum settlement in these small areas is amplified to some extent. In other words, the realistic maximum settlement in these small areas is smaller than that shown in Fig. 7c, d.

Clearly, in response to the 2 °C global warming, the permafrost degradation under the RCP4.5 scenario is

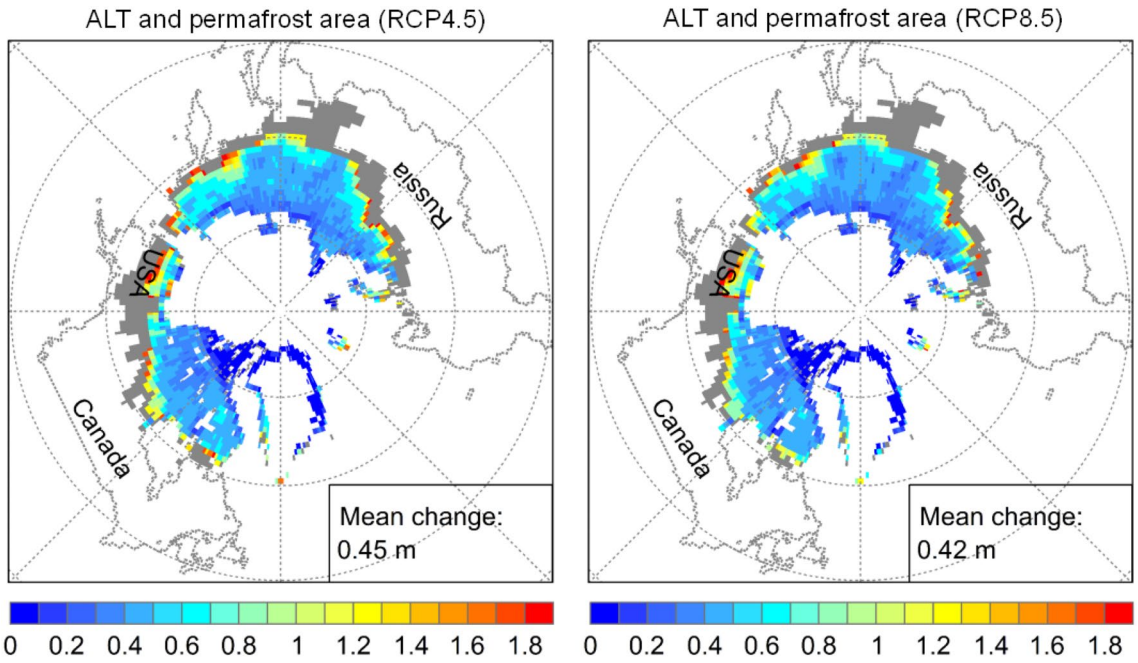

Fig. 6 Change in the active layer thickness (ALT) (m, *shaded color*) and permafrost area (*gray* area) between the 2 °C warming and 1990–2000 period under the RCP4.5 and RCP8.5 scenarios. Mean change denotes the area-averaged change. Three countries (Russia, Canada, and the USA), containing permafrost, are outlined by the *gray dashed lines*

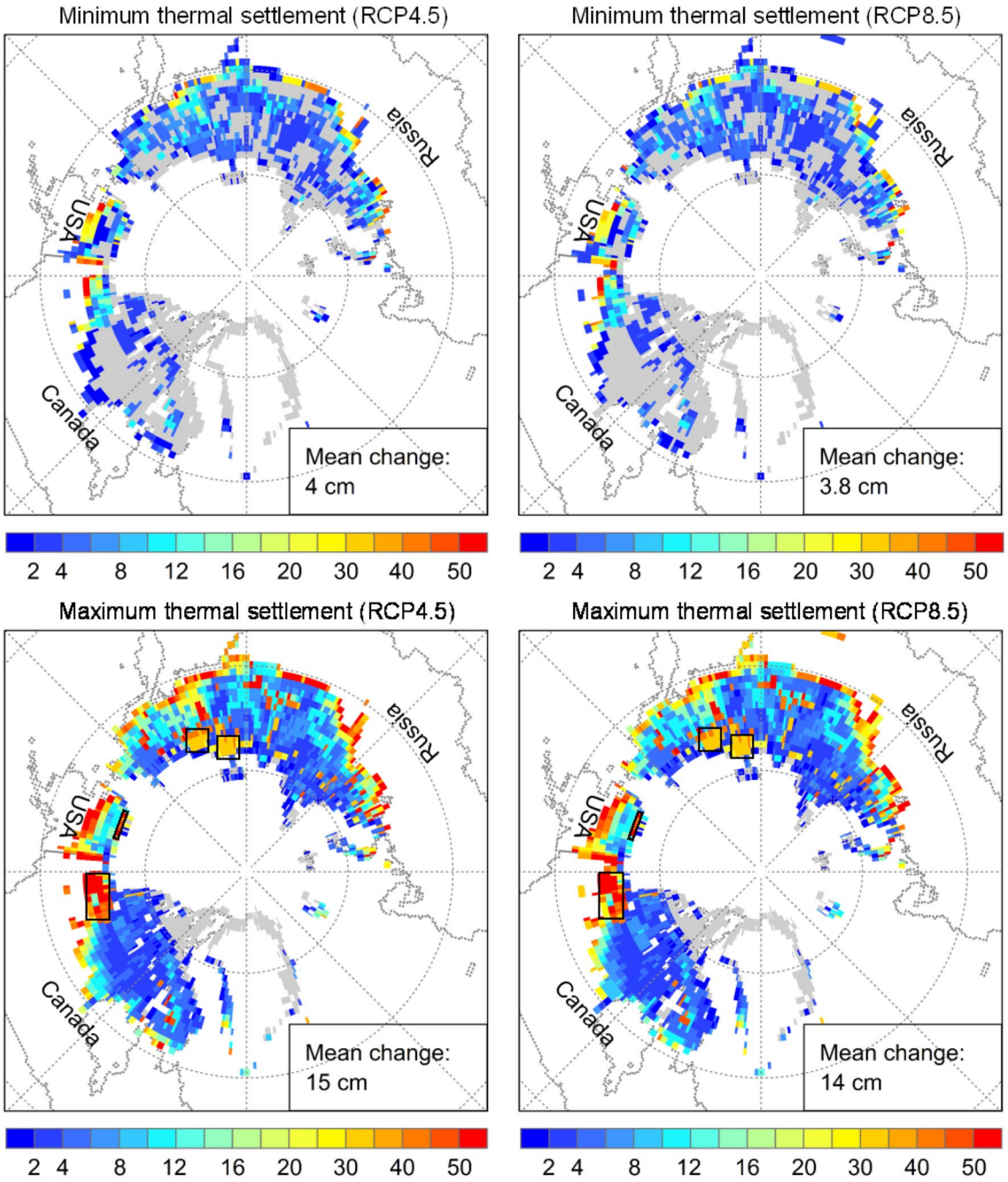

Fig. 7 Minimum and maximum settlement (cm) of the ground surface owing to permafrost thaw that is caused by the air temperature rise from 1990 to 2000 to the 2 °C warming period in the RCP4.5 and RCP8.5 scenarios. *Gray* areas represent the areas with the ground settlement below 1.0 cm. Mean change denotes the area-averaged change. Three countries (Russia, Canada, and the USA), containing permafrost, are outlined by the *gray dashed lines*

close to that under the RCP8.5 scenario. This is because these two scenarios behave similarly in the process of the 2 °C warming (Fig. 1). The small difference in permafrost degradation between the two scenarios may be due to slightly different time to reach the 2 °C warming (2037 for the RCP8.5 and 2045 for the RCP4.5, with a difference of 8 years). Generally, permafrost responds relatively slowly to changes in climate. More time (RCP4.5) could permit permafrost to respond more fully to the 2 °C global warming than less time (RCP8.5), which may cause the small difference.

4 Discussions

Assessing and quantifying permafrost thaw and associated settlement of the ground surface are important but very difficult due to generally poor ability of models to represent frozen ground-relevant processes such as snow, soil organic matter, and soil depth (Nicolsky et al. 2007; Koven et al. 2013). Nicolsky et al. (2007) indicated that the inclusion of soil organic matter and deeper soil layers significantly improved soil temperature simulation. Koven et al. (2013) demonstrated that snow cover plays a crucial role in permafrost simulation due to its insulation effect. This study chose the CMIP5 models with soil depth above 6 m. Moreover, the models include explicit frozen ground processes and multiple snow layers; most of the models also consider soil organic matter. These treatments are conducive to this simulation research.

Existing studies indicated that multi-model ensembles generally produces superior simulated results compared to individual models (e.g., Sillmann et al. 2013). The method has been widely used in climate simulation researches (Collins et al. 2013; Jiang et al. 2016). Accordingly, in this study, the multi-model ensemble method was used to expect reasonable results of estimation. Based on in situ site observations and the Circum-Arctic permafrost map, the simulated ensemble mean soil temperature, ALT, and permafrost area are validated. The statistical indices show that the simulated results are reasonable.

Differences in permafrost during the two periods (the 2 °C global warming and 1990–2000 period) are calculated to analyze the permafrost thaw and associated settlement of the ground surface in this study. When calculating the differences, systematical bias caused by some inherent factors such as computation inaccuracy and inappropriate resolution in the model can be removed, which makes the analysis results approach the true value. This means that the actual bias in the analysis results is smaller than that shown in the validation.

A source of possible uncertainties in this study is less accurate ground ice data. The ground ice data from the map of the Circum-Arctic permafrost and ground ice conditions are perhaps the best available data of ground ice distribution at the present. The data have been used to examine the risk zonation of thaw settlement hazard of permafrost (Nelson et al. 2002). But the data only provide a range of ground ice content for a model grid area, which results in estimating only the corresponding range of permafrost thaw-induced settlement of the ground surface. More observational studies of ground ice are expected in the future.

Although this study performs a choice of the CMIP5 models in terms of key processes (e.g., deeper soil and multiple snow layers) important for permafrost simulation, a few models still show weak ability to represent permafrost (Koven et al. 2013). This may contribute to part of possible uncertainties in the ensemble mean results in this study. More strict restrictions can be used for continued study; for example, to select the climate models with Community Land Model 4 (CLM4) as land surface model, which involves sophisticated permafrost-relevant processes (Oleson et al. 2010).

In addition, Burn and Nelson (2006) and Lawrence et al. (2008) indicated that inclusion of excess ground ice could delay the rate of permafrost thaw. But the models have not included the excess ground ice in their physical formulation. This may cause some of possible uncertainties in this simulation.

Besides, the relative coarser resolution (0.9° latitude × 1.125° longitude to 2.81° latitude × 2.81° longitude) of the models may be another source of possible uncertainties. The coarser resolution provides less regional information on climate change and makes the model difficult to capture regional details of permafrost change in response to the 2 °C global warming. A dynamical downscaling approach based on regional climate models can be used in the future to yield high-resolution permafrost data and possibly improve the estimations of permafrost degradation (Guo et al. 2012; Gao et al. 2013; Guo and Wang 2016a). Other factors, such as less accurate surface and soil texture data (Lawrence et al. 2008), may also contribute to at least part of possible uncertainties.

5 Summary

Permafrost thaw and associated ground settlement in response to the 2 °C global warming relative to the preindustrial climate were identified using soil temperature data from ten CMIP5 models and frozen ground observations. The area-averaged temperature over permafrost areas will increase by at least 2.9–4.4 °C when the globe will warm by 2 °C relative to preindustrial levels. The ensemble mean area of simulated present-day permafrost in the CMIP5 models agrees well with observational estimates. In situ site observations were also used to validate the simulated present-day soil temperature at depths of 1 and 6 m and the ALT. The simulation results were found reasonable.

The changes in the permafrost for the 2 °C global warming relative to the reference period of 1990–2000 were assessed. The soil temperature at depth of 6 m increases by 2.67 °C (RCP4.5) and 2.34 °C (RCP8.5); both are area means over the simulated present-day permafrost. The increase intensifies with increasing latitude. The ALT increases by 0.45 and 0.42 m on average under the RCP4.5 and RCP8.5 scenarios, respectively. The increase weakens with increasing latitude, a situation that is opposite to soil temperature. The permafrost

area displays an obvious northward retreat expressed by the relative decrease of 26 and 24% for RCP4.5 and RCP8.5, respectively. The ground settlement ranges from 4 to 15 cm (RCP4.5) and 3.8 to 14 cm (RCP8.5) with respect to area mean values. The settlement decreases with increasing latitude except for several small areas.

Despite the moderate target of 2 °C global warming relative to the preindustrial level, the results suggest significant permafrost thaw and associated ground settlement owing to the higher climate warming in the permafrost region than the global mean level. These results help to look at the 2 °C global warming target from the permafrost change perspective. Possible uncertainties in this study may be mostly related to the less accurate ground ice content data, which only provide a range of ground ice content. Another source of possible uncertainties may be due to absence of excess ground ice in the models, affecting the accuracy of the estimated results. Besides, the relatively coarser horizontal resolution and less accurate surface and soil texture data of the models also may contribute to part of possible uncertainties. More observation-based studies of ground ice in permafrost, inclusion of excess ground ice in the models and higher-resolution climate simulations are required in the future to minimize the possible uncertainties.

Historically, permafrost-relevant studies has moved from permafrost properties (e.g., Brown et al. 1997; Zhang et al. 1999; Romanovsky et al. 2010), to permafrost changes (e.g., Brown et al. 2000; Wu and Zhang 2008; Koven et al. 2013; Slater and Lawrence 2013; Guo and Wang 2016b), and then to the impacts of permafrost change on hydrology (e.g., Guo et al. 2012; Cuo et al. 2015; Liljedahl et al. 2016), ecosystems (e.g., Yang et al. 2010; Yi et al. 2014), and climate change (Schuur et al. 2009, 2015; Koven et al. 2011; Burke et al. 2013). This present study focuses on permafrost thaw-induced settlement of the ground surface. Furthermore, the growingly concerned scenario of the 2 °C global warming was used. Continued work will concentrate on permafrost thaw-induced ground settlement and the associated thermal hazard onset timing under multiple RCP scenarios, which may be based on the high-resolution output of the dynamical downscaling approach of regional climate models.

Acknowledgements This research was jointly supported by the National Key Research and Development Program of China (Grant No. 2016YFA0600704), the National Natural Science Foundation of China under Grants (41405087), the Open Research Fund Program of Plateau Atmosphere and Environment Key Laboratory of Sichuan Province under grant PAEKL-2016-K2, and the CAS-PKU Joint Research Program. Thanks are due to the Earth System Grid Federation (ESGF) that provided the CMIP5 simulation data (http://pcmdi9.llnl.gov/) and the National Snow & Ice data Center (NSIDC) that provided the Circum-Arctic map of permafrost and ground ice conditions (http://nsidc.org/data/docs/fgdc/ggd318_map_circumarctic/index.html). We are indebted to two reviewers for their constructive comments for the initial draft of this paper.

References

Anisimov OA, Nelson FE (1996) Permafrost distribution in the Northern Hemisphere under scenarios of climate change. Glob Planet Change 14:59–72

Anisimov OA, Nelson FE (1997) Permafrost zonation and climate change in the Northern Hemisphere: results from transient general circulation models. Clim Change 35:241–258

Anisimov OA, Reneva S (2006) Permafrost and changing climate: the Russian perspective. AMBIO 35:169–175

Anisimov OA, Fitzharris B, Hagan JO, Jeffries R, Marchant H, Nelson FE, Prowse T, Vaughan DG (2001) Polar regions (Arctic and Antarctic). In: McCarthy JJ et al (eds) Climate change 2001: impacts, adaptation, and vulnerability: contribution of working group II of the intergovernmental panel on climate change. Cambridge University Press, New York, pp 801–841

Bentsen M, Bethke I, Debernard JB, Iversen T, Kirkevåg A, Seland Ø, Drange H, Roelandt C, Seierstad IA, Hoose C, Kristjansson JE (2013) The Norwegian Earth System Model, NorESM1-M-Part 1: description and basic evaluation of the physical climate. Geosci Model Dev 6:687–720

Brown J, Ferrians OJ Jr, Heginbottom JA, Melnikov ES (1997) Circum-Arctic Map of Permafrost and Ground-Ice Conditions, U. S. Geological Survey in Cooperation with the Circum-Pacific Council for Energy and Mineral Resources, Circum-Pacific Map Series CP-45, scale 1:10,000, 000, 1 sheet

Brown J, Hinkel K, Nelson F (2000) The circumpolar active layer monitoring (CALM) program: research designs and initial results. Polar Geogr 24:165–258

Burke EJ, Jones CD, Koven CD (2013) Estimating the permafrost-carbon climate response in the CMIP5 climate models using a simplified approach. J Clim 26:4897–4909

Burn CR, Nelson FE (2006) Comment on "A projection of severe near-surface permafrost degradation during the 21st century" by David M. Lawrence and Andrew G. Slater. Geophys Res Lett 33:L21503. doi:10.1029/2006GL027077

Collins M, Knutti R, Arblaster J, Dufresne JL, Fichefet T, Friedlingstein P, Gao X, Gutowski WJ, Johns T, Krinner G, Shongwe M, Tebaldi C, Weaver AJ, Wehner M (2013) Long-term Climate Change: projections, commitments and irreversibility. In: Stocker TF et al (eds) Climate change 2013: the physical science basis. Contribution of working group I to the fifth assessment report of the intergovernmental panel on climate change. Cambridge University Press, Cambridge

Cuo L, Zhang Y, Bohn TJ, Zhao L, Li J, Liu Q, Zhou B (2015) Frozen soil degradation and its effects on surface hydrology in the northern Tibetan Plateau. J Geophys Res Atmos 120:8276–8298

Dunne JP, John JG, Adcroft AJ, Griffies SM, Hallberg RW, Shevliakova E, Stouffer RJ, Cooke W, et al (2012) GFDL's ESM2 global coupled climate–carbon Earth System Models. Part I: physical formulation and baseline simulation characteristics. J Clim 25:6646–6665

Gao XJ, Wang ML, Giorgi F (2013) Climate change over China in the 21st century as simulated by BCC_CSM1.1-RegCM4.0. Atmos Ocean Sci Lett 6:381–386

Gent PR, Danabasoglu G, Donner LJ, Holland MM, Hunke EC, Jayne SR, Lawrence DM, Neale RB, et al (2011) The community climate system model version 4. J Clim 24:4973–4991

Giannakopoulos C, Le Sager P, Bindi M, Moriondo M, Kostopoulou E, Goodess CM (2009) Climatic changes and associated impacts

in the Mediterranean resulting from a 2 °C global warming. Glob Planet Change 68:209–224
Gilichinsky D, Barry R, Bykhovets S, Sorokovikov V, Zhang T, Zudin S, Fedorov-Davydov D (1998) A century of temperature observations of soil climate: methods of analysis and long-term trends, Proc. Seventh Int. Conf. on Permafrost, Yellowknife, Northwest Territories. International Permafrost Association, Canada, pp 23–27
Giorgetta MA, Jungclaus J, Reick CH, Legutke S, Bader J, Böttinger M, Brovkin V, Crueger T, Coauthors (2013) Climate and carbon cycle changes from 1850 to 2100 in MPI-ESM simulations for the Coupled Model Intercomparison Project phase 5. J Adv Model Earth Syst 5:572–597
Guo DL, Sun JQ (2015) Permafrost thaw and associated settlement hazard onset timing over the Qinghai-Tibet engineering corridor. Int J Disaster Risk Sci 6:347–358
Guo DL, Wang HJ (2012) The significant climate warming in the northern Tibetan Plateau and its possible causes. Int J Climatol 32:1775–1781
Guo DL, Wang HJ (2013) Simulation of permafrost and seasonally frozen ground conditions on the Tibetan Plateau, 1981–2010. J Geophys Res Atmos 118:5216–5230
Guo DL, Wang HJ (2014) Simulated change in the near-surface soil freeze/thaw cycle on the Tibetan Plateau from 1981 to 2010. Chin Sci Bull 59:2439–2448
Guo DL, Wang HJ (2016a) Comparison of a very-fine-resolution GCM and RCM dynamical downscaling in simulating climate in China. Adv Atmos Sci 33:559–570
Guo DL, Wang HJ (2016b) CMIP5 permafrost degradation projection: s comparison among different regions. J Geophys Res Atmos 121:4499–4517
Guo DL, Yang MX, Wang HJ (2011a) Characteristics of land surface heat and water exchange under different soil freeze/thaw conditions over the central Tibetan Plateau. Hydrol Process 25:2531–2541
Guo DL, Yang MX, Wang HJ (2011b) Sensible and latent heat flux response to diurnal variation in soil surface temperature and moisture under different freeze/thaw soil conditions in the seasonal frozen soil region of the central Tibetan Plateau. Environ Earth Sci 63:97–107
Guo DL, Wang HJ, Li D (2012) A projection of permafrost degradation on the Tibetan Plateau during the 21st century. J Geophys Res 117:D05106. doi:10.1029/2011JD016545
Hartmann DL, Klein Tank AMG, Rusticucci M, Alexander LV, Brönnimann S, Charabi Y, Dentener FJ, Dlugokencky EJ, Easterling DR, Kaplan A, Soden BJ, Thorne PW, Wild M, Zhai PM (2013) Observations: Atmosphere and Surface. In: Stocker TF et al (eds) Climate change 2013: the physical science basis. Contribution of working group I to the fifth assessment report of the intergovernmental panel on climate change. Cambridge University Press, Cambridge
Hua WJ, Chen HS, Sun SL (2014) Uncertainty in land surface temperature simulation over China by CMIP3/CMIP5 climate models. Theor Appl Climatol 117:363–474
James WH, Holland MM, Gent PR, Ghan S, Kay JE, Kushner PJ, Lamarque JF, Large WG, et al (2013) The Community Earth System Model: a framework for collaborative research. Bull Am Meteorol Soc 94:1339–1360
Jiang DB, Fu YH (2012) Climate change over China with a 2 °C global warming. Chin. J Atmos Sci 36:234–246 (**Chinese**)
Jiang DB, Sui Y, Lang X (2016) Timing and associated climate change of a 2 °C global warming. Int J Climatol. doi:10.1002/joc.4647
Kaplan JO, New M (2006) Arctic climate change with a 2 °C global warming: timing, climate patterns and vegetation change. Clim Change 79:213–241
Koven CD, Ringeval B, Friedlingstein P, Ciais P, Cadule P, Khvorostyanov D, Krinner G, Tarnocai C (2011) Permafrost carbon-climate feedbacks accelerate global warming. Proc Natl Acad Sci 108:14769–14774
Koven CD, Riley WJ, Stern A (2013) Analysis of permafrost thermal dynamics and response to climate change in the CMIP5 Earth System Models. J Clim 26:1877–1900
Lan C, Zhang YX, Bohn TJ, Zhao L, Li JL, Liu QM, Zhou BR (2015) Frozen soil degradation and its effects on surface hydrology in the northern Tibetan Plateau. J Geophys Res Atmos 120:8276–8298
Lang XM, Sui Y (2013) Changes in mean and extreme climates over China with a 2 °C global warming. Chin Sci Bull 58:1453–1461
Lawrence DM, Slater AG, Romanovsky VE, Nicolsky DJ (2008) Sensitivity of a model projection of near-surface permafrost degradation to soil column depth and representation of soil organic matter. J Geophys Res. doi:10.1029/2007JF000883
Lawrence DM, Oleson KW, Flanner MG, Thornton PE, Swenson SC, Lawrence PJ, Zeng XB, Yang ZL, Levis S, Sakaguchi K, Bonan GB, Slater AG (2011) Parameterization improvements and functional and structural advances in version 4 of the Community Land Model. J Adv Model Earth Syst. doi:10.1029/2011MS000045
Lawrence DM, Slater AG, Swenson SC (2012) Simulation of present-day and future permafrost and seasonally frozen ground conditions in CCSM4. J Clim 25:2207–2225
Li Q, Chen HS (2013) Variation of seasonal frozen soil in East China and their association with monsoon activity under the background of global warming. Clim Change Res Lett 2:47–53 (in Chinese)
Li F, Wang HJ, Gao YQ (2015) Change in sea ice cover is responsible for non-uniform variation in winter temperature over East Asia. Atmos Oceanic Sci Lett 8:376–382
Liljedahl AK, Boike J, Daanen RP, Fedorov AN, Frost GV, Grosse G, Hinzman LD, Iijma Y, Jorgenson JC, Matveyeva N, Necsoiu M, Raynolds MK, Romanovsky VE, Schulla J, Tape KD, Walker DA, Wilson CJ, Yabuki H, Zona D (2016) Pan-Arctic ice-wedge degradation in warming permafrost and its influence on tundra hydrology. Nat Geosci 9:312–318
Liu Y, Jiang D (2016) Mid-Holocene permafrost: Results from CMIP5 simulations. J Geophys Res Atmos 121:221–240
Liu J, Curry JA, Wang HJ, Song M, Horton RM (2012) Impact of declining Arctic sea ice on winter snowfall. Proc Natl Acad Sci 109:4074–4079
May W (2012) Assessing the strength of regional changes in near-surface climate associated with a global warming of 2 °C. Clim Change 110:619–644
Meinshausen M, Meinshausen N, Hare W, Raper SCB, Frieler K, Knutti R, Frame DJ, Allen MR (2009) Greenhouse-gas emission targets for limiting global warming to 2 °C. Nature 458:1158–1162
Moss RH, Edmonds JA, Hibbard KA, Manning MR, Rose SK, Vuuren D, Timothy R, Emori S, Coauthors (2010) The next generation of scenarios for climate change research and assessment. Nature 463:747–756
Nelson FE, Anisimov OA, Shiklomanov NI (2001) Subsidence risk from thawing permafrost. Nature 410:889–890
Nelson FE, Anisimov OA, Shiklomanov N (2002) Climate change and hazard zonation in the circum-Arctic permafrost regions. Nat Hazards 26:203–225
Nicolsky DJ, Romanovsky VE, Alexeev VA, Lawrence DM (2007) Improved modeling of permafrost dynamics in a GCM land-surface scheme. Geophys Res Lett 34:L08501. doi:10.1029/2007GL029525
Oleson K, Lawrence D, Bonan G, Flanner M, Kluzek E, Lawrence P, Levis S, Swenson S, Thornton P, Dai A, Decker M, Dickinson

R, Feddema J, Heald C, Hoffman F, Lamarque J, Mahowald N, Niu G, Qian T, Randerson J, Running S, Sakaguchi K, Slater A, Stöckli R, Wang A, Yang Z, Zeng X, Zeng X 2010 Technical description of version 4.0 of the community land model (CLM). NCAR technical note NCAR/TN-478+STR. National Center for Atmospheric Research, Boulder, PP 266

Qin DH, Zhou BT, Xiao CD (2014) Progress in studies of cryospheric changes and their impacts on climate of China. J Meteorol Res 28:732–746

Romanovsky (2010) Development of a network of permafrost observatories in North America and Russia: the US contribution to the international polar year. Advanced Cooperative Arctic Data and Information Service, Boulder, (digital media)

Romanovsky VE, Smith SL, Christiansen HH (2010) Permafrost thermal state in the polar Northern Hemisphere during the international polar year 2007–2009: a synthesis. Permafr Periglac Process 21:106–116

Schneider SH, Semenov S, Patwardhan A, Burton I, Magadza CHD, Oppenheimer M, Pittock AB, Rahman A, Smith JB, Suarez A, Yamin F (2007) Assessing key vulnerabilities and the risk from climate change, climate change 2007: impacts, adaptation and vulnerability. Contribution of working group II to the fourth assessment report of the intergovernmental panel on climate change. Parry ML, Canziani OF, Palutikof JP, van der Linden PJ, Hanson CE (eds) Cambridge University Press, Cambridge, pp 779–810

Schuur E, Vogel J, Crummer K, Lee H, Sickman J, Osterkamp T (2009) The effect of permafrost thaw on old carbon release and net carbon exchange from tundra. Nature 459:556–559

Schuur E, McGuire AD, Schädel C, Grosse G, Harden JW, Hayes DJ, Hugelius G, Koven CD, Kuhry P, Lawrence DM, Natali SM, Olefeldt D, Romanovsky VE, Schaefer K, Turetsky MR, Treat CC, Vonk JE (2015) Climate change and the permafrost carbon feedback. Nature 520:171–179

Sillmann J, Kharin VV, Zhang X, Zwiers FW, Bronaugh D (2013) Climate extremes indices in the CMIP5 multimodel ensemble: Part 1. Model evaluation in the present climate. J Geophys Res Atmos 118:1716–1733

Slater AG, Lawrence DM (2013) Diagnosing present and future permafrost from climate models. J Clim 26:5608–5623

Stendel M, Christensen J (2002) Impact of global warming on permafrost conditions in a coupled GCM. Geophys Res Lett 29:1632. doi:10.1029/2001GL014345

Sui Y, Lang X, Jiang D (2015) Temperature and precipitation signals over China with a 2 °C global warming. Clim Res 64:227–242

Takata K, Emori S, Watanabe T (2003) Development of the minimal advanced treatments of surface interaction and runoff. Glob Planet Change 38:209–222

Taylor KE, Stouffer RJ, Meehl GA (2012) An overview of CMIP5 and the experiment design. Bull Am Meteor Soc 93:485–498

Tjiputra JF, Roelandt C, Bentsen M, Lawrence DM, Lorentzen T, Schwinger J, Seland Ø, Heinze C (2013) Evaluation of the carbon cycle components in the Norwegian Earth System Model (NorESM). Geosci Model Dev 6:301–325

UNFCCC (2010) The Cancun Agreements United Nations Framework Convention on Climate Change. http://unfccc.int/meetings/cancun nov 2010/meeting/6266.php

UNFCCC (2015) The Paris Agreements United Nations Framework Convention on Climate Change. http://unfccc.int/documentation/documents/advanced_search/items/6911.php?priref=600008831

Vautard R, Gobiet A, Sobolowski S, Kjellstrom E, Stegehuis A, Watkiss P, Mendlik T, Landgren O, Nikulin G, Teichmann C, Jacob D (2014) The European climate under a 2 °C global warming. Environ Res Lett 9:034006

Wang HJ, Sun JQ (2009) Variability of Northeast China River Breakup Date. Adv Atmos Sci 26:701–706

Wang HJ, Chen HP, Liu J (2015) Arctic sea ice decline intensified haze pollution in eastern China. Atmos Ocean Sci Lett 8:1–9

Watanabe M, Suzuki T, O'ishi R, Komuro Y, Watanabe S, Emori S, Coauthors (2010) Improved climate simulation by MIROC5: mean states, variability, and climate sensitivity. J Clim 23:6312–6335

Watanabe S, Hajima T, Sudo K, Nagashima T, Takemura T, Okajima H, Coauthors (2011) MIROC-ESM 2010: model description and basic results of CMIP5-20c3m experiments. Geosci Model Dev 4:845–872

Wu QB, Zhang TJ (2008) Recent permafrost warming on the Qinghai-Tibetan Plateau. J Geophys Res 113:D13108. doi:10.1029/2007JD009539

Wu QB, Zhang TJ, Liu YZ (2010) Permafrost temperatures and thickness on the Qinghai-Tibet Plateau. Glob Planet Change 72:32–38

Xu XZ, Wang JC, Zhang LX (2010) Physics of frozen soil, 2nd edn. Science Press, Beijing, (in Chinese)

Yang MX, Nelson F, Shiklomanov N, Guo DL, Wan G (2010) Permafrost degradation and its environmental effects on the Tibetan Plateau: a review of recent research. Earth-Sci Rev 103:31–44

Yang K, Wu H, Qin J, Lin C, Tang W, Chen Y (2014) Recent climate changes over the Tibetan Plateau and their impacts on energy and water cycle: a review. Glob Planet Change 112:79–91

Yi S, Wang X, Qin Y, Xiang B, Ding Y (2014) Responses of alpine grassland on Qinghai–Tibetan plateau to climate warming and permafrost degradation: a modeling perspective. Environ Res Lett 9:074014

Yukimoto S, Adachi Y, Hosaka M, Sakami T, Yoshimura H, Hirabara M, Tanaka TY, Shindo E, Coauthors (2012) A new global climate model of the Meteorological Research Institute: MRI-CGCM3—model description and basic performance. J Meteorol Soc Japan 90A:23–64

Zhang Z, Wu Q (2012) Thermal hazards zonation and permafrost change over the Qinghai-Tibet Plateau. Nat hazard 61:403–423

Zhang T, Barry RG, Knowles K, Heginbottom JA, Brown J (1999) Statistics and characteristic of permafrost and ground-ice distribution in the Northern Hemisphere. Polar Geogr 23:132–154

Zhang T, Barry R, Gilichinsky D (2001) Russian historical soil temperature data, National Snow and Ice Data Center, Boulder, (digital media)

Zhang T, Frauenfeld OW, Barry RG (2006) Time series of active layer thickness in the Russian Arctic, 1930–1990, National Snow and Ice Data Center, Boulder, (digital media)

Zhang Y, Chen W, Riseborough DW (2008) Transient projections of permafrost distribution in Canada during the 21st century under scenarios of climate change. Glob Planet Change 60:443–456

Zhou BT, Wen QH, Xu Y, Song LC, Zhang XB (2014) Projected changes in temperature and precipitation extremes in China by the CMIP5 multi-model ensembles. J Clim 27:6591–6611

Zhou BT, Xu Y, Wu J, Dong S, Shi Y (2016) Changes in temperature and precipitation extreme indices over China: analysis of a high-resolution grid dataset. Int J Climatol 36:1051–1066

Zimov S, Schuur E, Chapin F III (2006) Permafrost and the global carbon budget. Science 312:1612–1613